



Temperature and field induced strain in polycrystalline $\text{Ni}_{50}\text{Mn}_{35}\text{In}_{15-x}\text{Si}_x$ magnetic shape memory Heusler alloys

Arjun K. Pathak^{a,*}, Igor Dubenko^a, Shane Stadler^b, Naushad Ali^a

^a Department of Physics, Southern Illinois University, Carbondale, IL 62901, USA

^b Department of Physics and Astronomy, Louisiana State University, Baton Rouge, LA 70803, USA

ARTICLE INFO

Article history:

Received 16 August 2010

Accepted 4 September 2010

Available online 28 October 2010

Keywords:

Shape memory
Heusler alloys

ABSTRACT

Magnetic shape memory properties of polycrystalline $\text{Ni}_{50}\text{Mn}_{35}\text{In}_{15-x}\text{Si}_x$ were investigated. A reversible strain of more than 0.4% was observed for $x = 0$ at a magnetic field $H = 5$ T that was found to be associated with a field induced reverse martensitic transformation. The strains were found to increase with the substitution of In by Si and strains larger than 1% were observed for $x = 2$ at $H = 5$ T. Both the positive and negative strain changes were observed in the vicinity of martensitic transition temperatures. The strain in $\text{Ni}_{50}\text{Mn}_{35}\text{In}_{15-x}\text{Si}_x$ was found to depend on silicon concentration, and on samples texture.

© 2010 Elsevier B.V. All rights reserved.

1. Introduction

Ni–Mn–X (X = In, Sb, Sn, Ga) based Heusler alloys are multifunctional magnetic materials that exhibit several interesting properties such as giant magnetocaloric and shape memory effects, magnetoresistance, and exchange bias [1–7]. These materials show a ferromagnetic shape memory effects and hence the shape of the materials can be controlled using a magnetic field. The giant temperature or magnetic field induced magnetoelastic strains are an intrinsic property of the Ni–Mn–X based Heusler alloys [8,9]. Such compounds are sought for use in applications that range from magnetic actuators to low frequency active vibration damping systems. The study of magnetically induced strains in these multifunctional Heusler alloys can give more insight into the role of magnetoelastic properties in magnetic behavior of the materials.

Large strains of about 3% and 1% were observed in the martensitic phase of pre-strain samples of single crystals $\text{Ni}_{45}\text{Co}_5\text{Mn}_{36.7}\text{In}_{13.3}$ [10] and polycrystalline $\text{Ni}_{43}\text{Co}_7\text{Mn}_{39}\text{Sn}_{11}$ [8], respectively. Similarly, with out pre-strain about 0.1% strain was reported in the vicinity of martensitic transition for polycrystalline Ni–Mn–In [9,11]. It was shown in Ref. [12] that strength of strain depends upon the columnar grain direction of sample in the study of polycrystalline $\text{Ni}_{45.2}\text{Mn}_{36.7}\text{In}_{13}\text{Co}_{5.1}$. Taking into account the lack of experimental data concerning the factors affecting the magnetoelastic properties of magnetic Heusler alloys, the study of field and temperature induced strains in the Ni–Mn–In based compounds are of acute interest from both scientific and application points of view.

Recently, it was reported that $\text{Ni}_{50}\text{Mn}_{35}\text{In}_{15}$ is a ferromagnetic material that undergoes at least three transitions: (i) at Curie temperature of martensitic phase (T_{CM}), (ii) the first-order structural martensitic transition at T_{M} , accompanied by a step-like variation in magnetic moment of the compound; and (ii) the ferromagnetic–paramagnetic transition at the Curie temperature (T_{C}) of the austenitic phase ($T_{\text{CM}} < T_{\text{M}} < T_{\text{C}}$) [2,3]. The partial substitution of In by Si (in $\text{Ni}_{50}\text{Mn}_{35}\text{In}_{15-x}\text{Si}_x$) results in increase of jump in magnetization at the martensitic transition with respect to temperature and, an enhanced giant magnetocaloric effect [13]. Taking into account that magnetoelastic coupling is responsible for the shape memory effect in the compounds; the large strain anomaly associated with field/temperature induced magneto-structural transition is expected in this system.

In this work we explored the magnetoelastic properties of $\text{Ni}_{50}\text{Mn}_{35}\text{In}_{15-x}\text{Si}_x$ through X-ray diffraction (XRD), strain, and magnetization measurements. The temperature- and fields-induced anomaly in strain observed in $\text{Ni}_{50}\text{Mn}_{35}\text{In}_{15-x}\text{Si}_x$ system in vicinity of magneto-structural transitions was found to depend on composition and on samples texture.

2. Experimental techniques

Approximately 5 g polycrystalline $\text{Ni}_{50}\text{Mn}_{35}\text{In}_{15-x}\text{Si}_x$ ($0 \leq x \leq 4$) ingots were fabricated by a method described in Ref. [13]. The phase purity and crystal structures were determined by powder X-ray diffraction using Cu K α radiation. Prior to magnetization and strain measurements, the samples were cooled down under a zero external magnetic fields from above the Curie temperature of the austenitic phase (380 K). The magnetic properties were measured using a SQUID magnetometer (Quantum Design, Inc.). For strain measurements, the samples were cut (i) parallel and (ii) perpendicular to the direction of sample solidification during arc melting. We respectively called the samples as type I and type II. The temperature and field induced strain both parallel and perpendicular to the external

* Corresponding author. Tel.: +1 6184537126; fax: +1 6184531056.

E-mail address: pathak@siu.edu (A.K. Pathak).

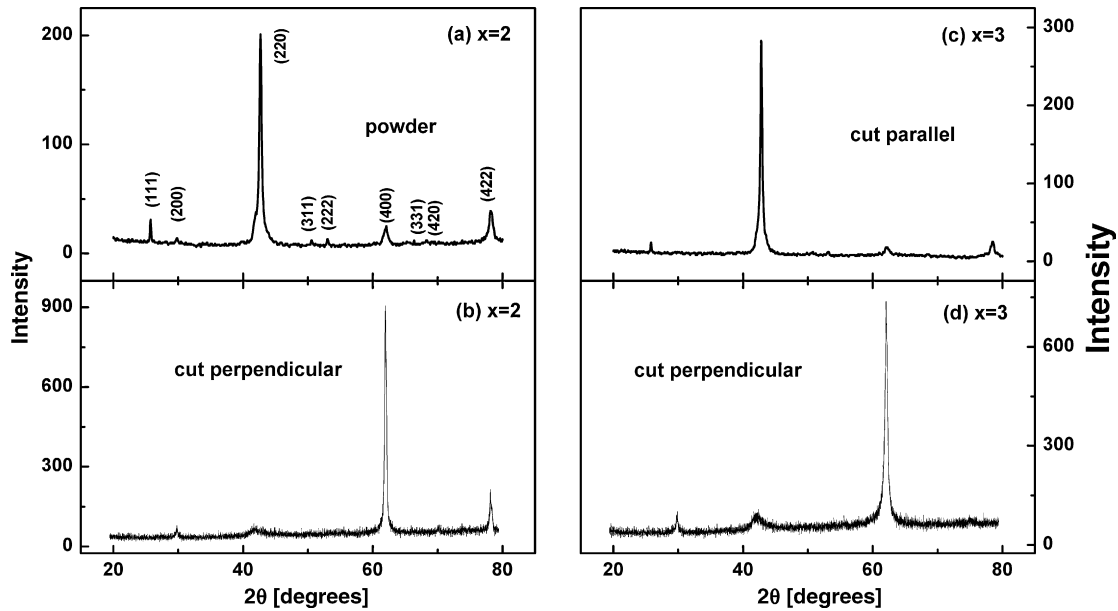


Fig. 1. (a–d) Room temperature X-ray diffraction patterns for powder sample, cut parallel and perpendicular to the direction of sample solidification during arc melting for $\text{Ni}_{50}\text{Mn}_{35}\text{In}_{15-x}\text{Si}_x$ ($x = 2$ and 3).

magnetic field directions were measured using a strain gauge in magnetic fields up to 5 T. The possible grain texture (preferable orientation of the grains) was studied by XRD diffraction at room temperature using bulk samples (type I and II). The samples were rolled at several angles and average XRD patterns were taken.

3. Results and discussion

The crystal structure of $\text{Ni}_{50}\text{Mn}_{35}\text{In}_{15-x}\text{Si}_x$ at room temperature depends on x , and varies from a martensitic orthorhombic

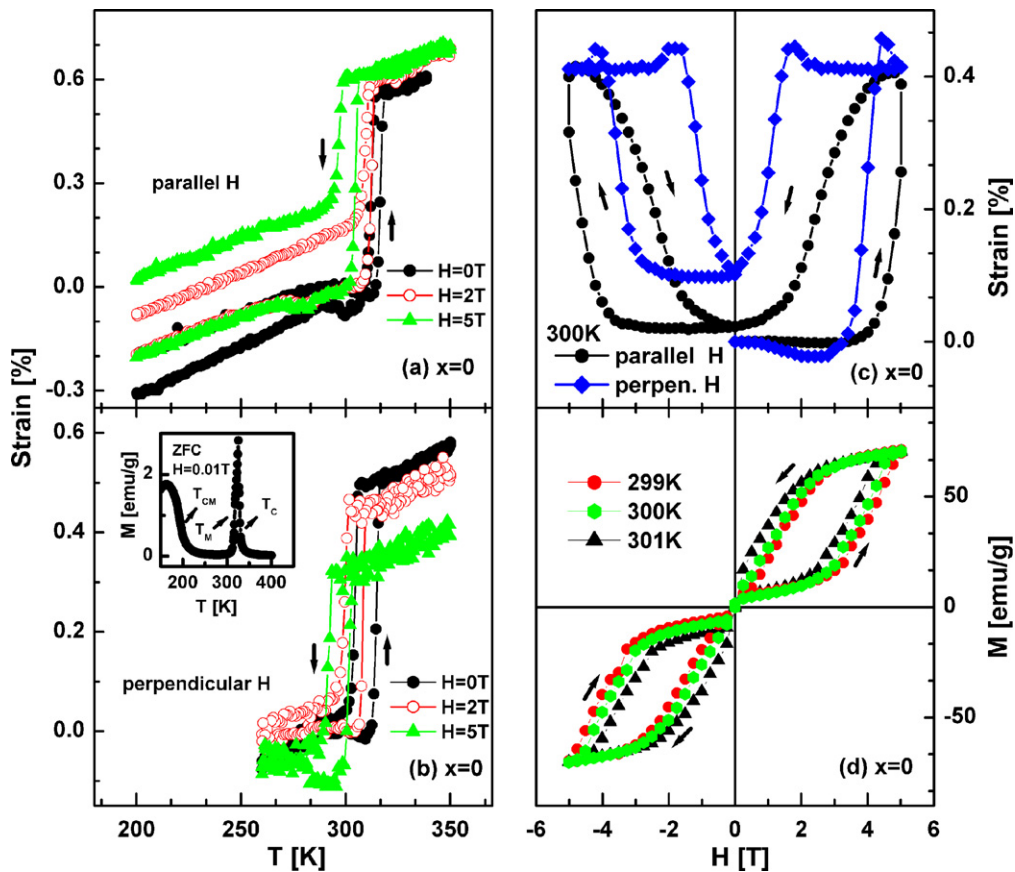


Fig. 2. Temperature dependence of the strain for $\text{Ni}_{50}\text{Mn}_{35}\text{In}_{15}$ measured in (a) parallel and (b) perpendicular to the direction of applied field. (c) The field dependence of the strain for $\text{Ni}_{50}\text{Mn}_{35}\text{In}_{15}$ measured in parallel (circles) and perpendicular (diamonds) to the direction of applied field. (d) Isothermal magnetization hysteresis curves for $\text{Ni}_{50}\text{Mn}_{35}\text{In}_{15}$ measured in the vicinity of martensitic transition.

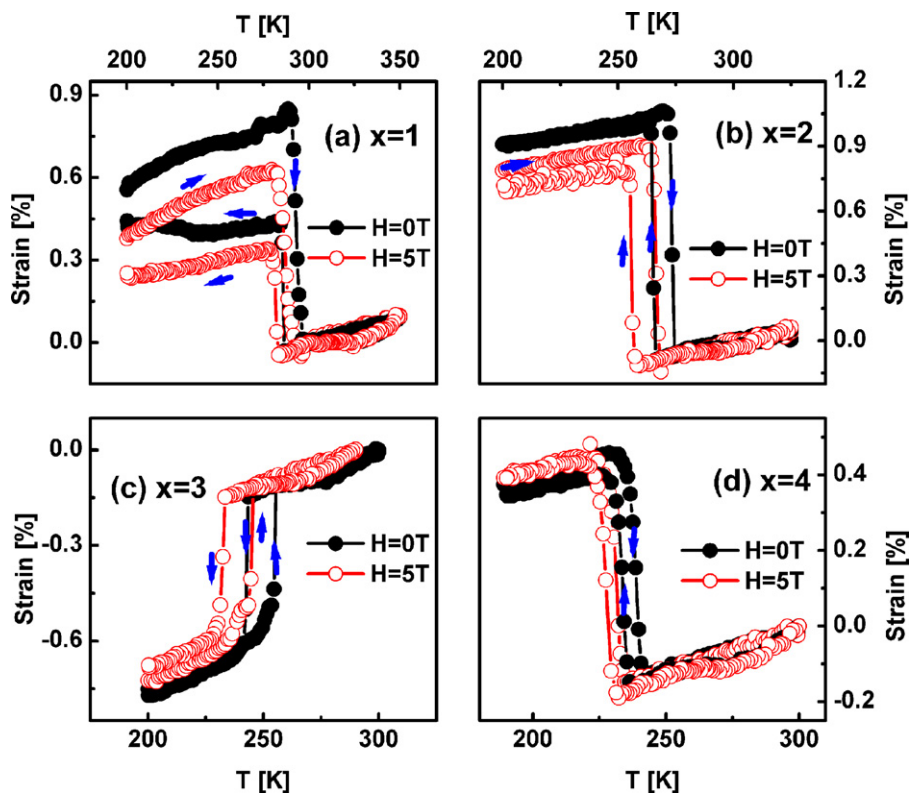


Fig. 3. (a–d) Temperature dependence of the strain measured parallel to the external magnetic field of zero and 5 T for $\text{Ni}_{50}\text{Mn}_{35}\text{In}_{15-x}\text{Si}_x$.

structure for $x=0$ to an austenitic cubic phase for $x \geq 1$ [6,13]. Room-temperature XRD patterns for bulk $\text{Ni}_{50}\text{Mn}_{35}\text{In}_{15-x}\text{Si}_x$ with $x=2$ and 3 (types I and II) and powder $x=2$ sample are shown in Fig. 1. It can be seen from the figure that the crystalline

grains have a preferable orientation relative to sample solidification axis. The grains are basically oriented along $\{h00\}$ and $\{hk0\}$, $h=k$ direction for samples of types I and II, respectively. Thus Si-doped $\text{Ni}_{50}\text{Mn}_{35}\text{In}_{15-x}\text{Si}_x$ are textured and observed texture

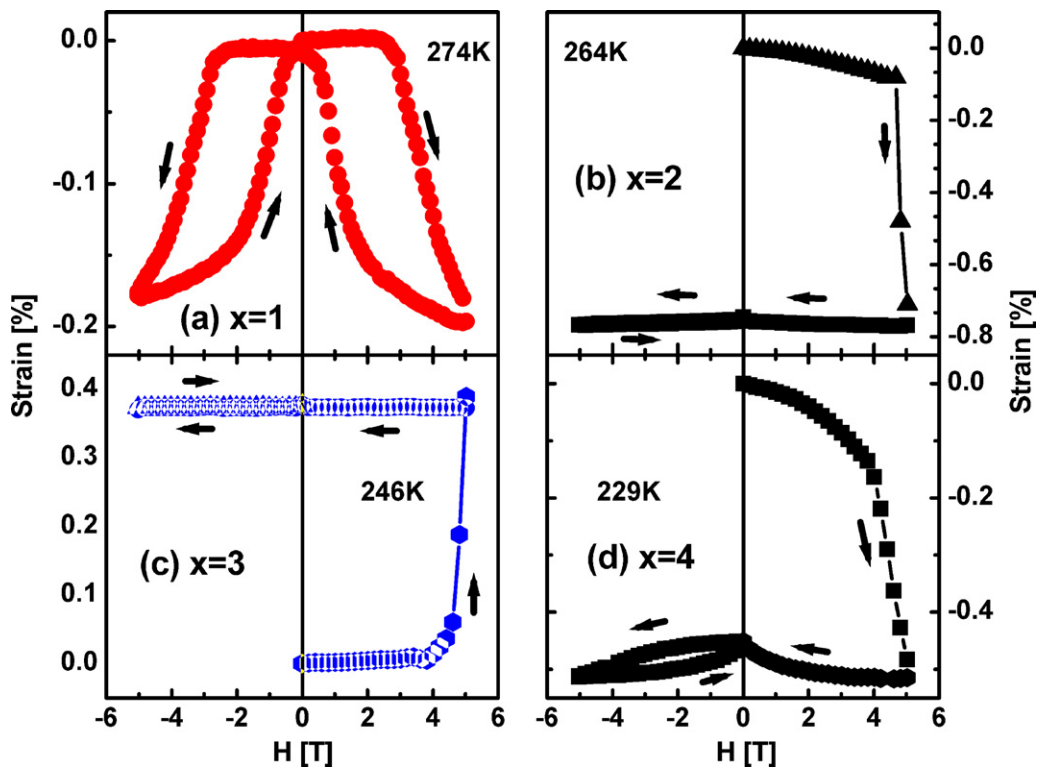


Fig. 4. (a–d) Field dependence of the strain measured parallel to the external magnetic field for $\text{Ni}_{50}\text{Mn}_{35}\text{In}_{15-x}\text{Si}_x$.

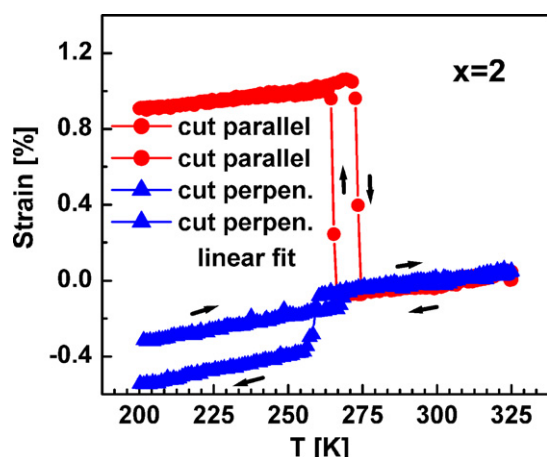


Fig. 5. Temperature dependence of the strain measured parallel to the external magnetic field for the sample cut parallel and perpendicular to the direction of sample solidification during arc melting for $\text{Ni}_{50}\text{Mn}_{35}\text{In}_{13}\text{Si}_2$.

can affect magneto-elastic behaviors of Ni–Mn–X polycrystalline materials.

The temperature dependence of the strains measured parallel and perpendicular to the external magnetic fields for $\text{Ni}_{50}\text{Mn}_{35}\text{In}_{15}$ for a type I sample are shown in Fig. 2(a) and (b). The strain increases with increasing temperature and shows a sharp jump ($\approx 0.6\%$) in the vicinity of T_M (see inset of Fig. 2(b) for $M(T)$ curves). This value of strain is higher than that found in polycrystalline Ni–Mn–X ($X = \text{Sb, Sn, In, Ga}$) [9,11,12]. The strain in both parallel and perpendicular (to H) directions show almost similar changes, indicating the isotropic character of this system. As shown in Fig. 2(a) and (b), the jump in strain slightly decreases with increasing external magnetic fields. Similar behavior was also reported by Aksoy et al. [9]. The jump-like strain changes, large temperature hysteresis, and shift of T_M towards lower temperature were resulted from a field induced reverse martensitic transformation. The magnetic field dependence strain at $T = 300 \text{ K} \leq T_M$ is shown in Fig. 2(c). The strain remains relatively unchanged until the applied field reaches a critical value, and a sharp increase in strain of up to $\approx 0.4\%$ was observed for $H = 5 \text{ T}$. The initial value of strain was recovered after the removal of the field in all field cycles, for both parallel and perpendicular field orientations (see Fig. 2(c)). The strain changes of 0.4% obtained without applying the

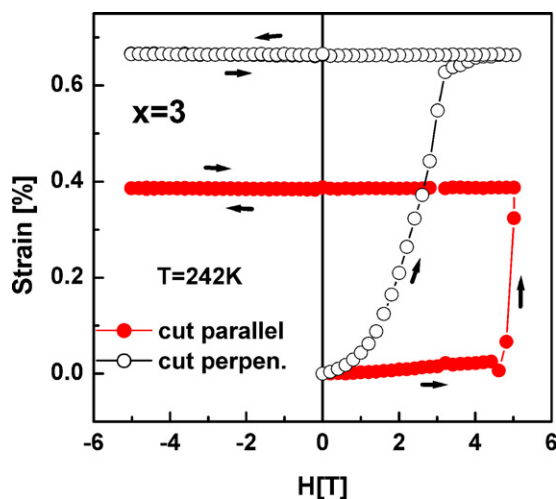


Fig. 6. Field dependence of the strain measured parallel to the external magnetic field for the sample cut parallel and perpendicular to the direction of sample solidification during arc melting for $\text{Ni}_{50}\text{Mn}_{35}\text{In}_{12}\text{Si}_3$.

prestrain is significantly higher than that recently reported for polycrystalline Ni–Mn–X ($X = \text{In, Sb, Sn, Ga}$) [for examples, $\approx 0.1\%$ in Ref [14], and $\approx 0.2\%$ in Ref. [9]]. Fig. 2(d) shows the isothermal magnetization curves in the vicinity of T_M . The curves show metamagnetic behavior with a field hysteresis of $\approx 2 \text{ T}$, which is similar to that observed in the strain measurements. Considering that the application of a magnetic field results in an increase in the fraction of austenitic phase, the observed strain changes are due to a magnetic field induced, reverse transformation from the antiferromagnetic martensite to the ferromagnetic parent phase.

Fig. 3 shows the temperature dependent strain for Si substituted $\text{Ni}_{50}\text{Mn}_{35}\text{In}_{15-x}\text{Si}_x$ with $x \leq 4$ for type I samples. As it can be seen from Fig. 3, negative volume anomalies were observed for $x = 1, 2$, and 4 , while a positive volume anomaly was observed for $x = 3$, as in the case of parent compounds ($x = 0$). The maximum jump in strain of more than 1% was observed for $x = 2$ in the vicinity of T_M , and volume anomalies were found to decrease with increasing in applied fields. The positive and negative volume changes in Si doped $\text{Ni}_{50}\text{Mn}_{35}\text{In}_{15-x}\text{Si}_x$ was also confirmed by field strain measurements (see Fig. 4), where a giant value of the shape memory effect was observed. Similar signs of volume anomalies (both positive and negative) were also reported in Refs. [12,15]. In order to investigate the possible physical origins of the positive and negative volume anomalies, we measured the strain in the parallel field direction for a type II sample. The results are shown in Fig. 5. Interestingly, when the strain was measured for a type II sample, the positive volume anomaly was also observed for $x = 2$. The field dependence of the strain for $x = 3$ at $T = 242 \text{ K}$ for both samples (types I and II) are presented in Fig. 6. It can be concluded from Fig. 6 that the strain behavior in $\text{Ni}_{50}\text{Mn}_{35}\text{In}_{15-x}\text{Si}_x$ strongly depends on the direction of strain gauge orientation relative to the sample texture (solidification) axis.

4. Conclusion

In conclusion, we have studied the magnetic shape memory effects in polycrystalline $\text{Ni}_{50}\text{Mn}_{35}\text{In}_{15-x}\text{Si}_x$. A reversible shape memory effect with a strain as large as 0.4% was observed at room temperature at a magnetic field of 5 T for $x = 0$. The sign of the volume anomaly at T_M , and the magnitude of the strains were found to depend on sample textures. A significantly large strain with a maximum value of about $\approx 1\%$ was found for $x = 2$ at $H = 5 \text{ T}$ (without applying the prestrain). In addition to giant strains, giant values of the magnetocaloric effect, large magnetoresistance, and exchange bias effects have been observed in $\text{Ni}_{50}\text{Mn}_{35}\text{In}_{15-x}\text{Si}_x$. Collectively, these properties make the systems potential materials for multifunctional application.

Acknowledgements

This research was supported by the Research Opportunity Award from Research Corporation (RA-0357) and by the Office of Basic Energy Sciences, Material Sciences Division of the U. S. Department of Energy (Contact No. DE-FGP2-06ER46291).

References

- [1] V.V. Khovaylo, K.P. Skokov, O. Gutfleisch, H. Miki, T. Takagi, T. Kanomata, V.V. Kolesov, V.G. Shavrov, G. Wang, E. Palacios, J. Bartolomé, R. Burriel, *Phys. Rev. B* 81 (2010) 214406.
- [2] S. Fabbri, F. Albertini, A. Paoluzi, F. Bolzoni, R. Cabassi, M. Solzi, L. Righi, G. Calestani, *Appl. Phys. Lett.* 95 (2009) 022508.
- [3] T. Krenke, E. Duman, M. Acet, E.F. Wassermann, X. Moya, L. Mañosa, A. Planes, E. Suard, B. Ouladif, *Phys. Rev. B* 75 (2007) 104414.
- [4] I. Dubenko, M. Khan, A.K. Pathak, B.R. Gautam, S. Stadler, N. Ali, *J. Magn. Magn. Mater.* 321 (2009) 754.
- [5] A.K. Pathak, I. Dubenko, S. Stadler, N. Ali, *J. Phys. D: Appl. Phys.* 42 (2009) 045004.
- [6] A.K. Pathak, M. Khan, I. Dubenko, S. Stadler, N. Ali, *Appl. Phys. Lett.* 90 (2007) 262504.

- [7] A.K. Pathak, M. Khan, B.R. Gautam, S. Stadler, I. Dubenko, N. Ali, J. Magn. Magn. Mater. 321 (2009) 963.
- [8] R. Kainuma, Y. Imano, W. Ito, H. Morita, Y. Sutou, K. Oikawa, A. Fujita, K. Ishida, S. Okamoto, O. Kitakami, T. Kanomata, Appl. Phys. Lett. 88 (2006) 192513.
- [9] S. Aksoy, T. Krenke, M. Acet, E.F. Wassermann, X. Moya, L. Mañosa, A. Planes, Appl. Phys. Lett. 91 (2007) 251915.
- [10] R. Kainuma, Y. Imano, W. Ito, Y. Sutou, H. Morito, S. Okamoto, O. Kitakami, K. Oikawa, A. Fujita, T. Kanomata, K. Ishida, Nature (London) 439 (2006) 957.
- [11] V.K. Sharma, M.K. Chattopadhyay, A. Chouhan, S.B. Roy, J. Phys. D: Appl. Phys. 42 (2009) 185005.
- [12] J. Liu, S. Aksoy, N. Scheerbaum, M. Acet, O. Gutfleisch, Appl. Phys. Lett. 95 (2009) 232515.
- [13] A.K. Pathak, I. Dubenko, S. Stadler, N. Ali, J. Phys. D: Appl. Phys. 41 (2008) 202004.
- [14] Z. Li, C. Jing, H.L. Zhang, Y.F. Qiao, S.X. Cao, J.C. Zhang, L. Sun, J. Appl. Phys. 106 (2009) 083908.
- [15] A.N. Vasil'ev, E.I. Estrin, V.V. Khovailo, A.D. Bozhko, R.A. Ischuk, M. Matsumoto, T. Takagi, J. Tani, Int. J. Appl. Electron. Mech. 12 (2000) 35.